Scattering of topological solitons on barriers and holes in two $\varphi^4$ models



2007 J. Phys. A: Math. Theor. 40 11319

(http://iopscience.iop.org/1751-8121/40/37/009)

IOP Publishing Journal of Physics A: Mathematical and Theoretical

J. Phys. A: Math. Theor. **40** (2007) 11319–11331 doi:10.1088/1751-8113/40/37/009

# Scattering of topological solitons on barriers and holes in two $\varphi^4$ models

**Jassem H Al-Alawi and Wojtek J Zakrzewski**

Department of Mathematical Sciences, University of Durham, Durham DH1 3LE, UK

E-mail: J.H.Al-Alawi@durham.ac.uk and W.J.Zakrzewski@durham.ac.uk

Received 5 July 2007, in final form 7 August 2007
Published 29 August 2007
Online at stacks.iop.org/JPhysA/40/11319

**Abstract**

We present the results of our studies of various scattering properties of topological solitons on obstructions in the form of holes and barriers in 1+1 dimensions. Our results are based on two models involving a $\varphi^4$ potential. The obstructions are characterized by a potential parameter, $\lambda$, which has a nonzero value in a certain region of space and zero elsewhere. In the first model the potential parameter is included in the potential and in the second model the potential parameter is included in the metric. Our results are based on numerical simulations and analytical considerations.

PACS numbers: 03.75.Lm, 05.45.Yv

## 1. Introduction

Some surprising aspects of the scattering of solitons have been attracting the attention of researchers and have been studied in many papers [1–3]. These studies have shown that a topological soliton behaves like a classical point particle when it is scattered on a potential barrier. In such a case the soliton follows a well-defined trajectory and as it meets the barrier it slows down and, if it has enough energy to 'climb' over the barrier, it gets transmitted otherwise it gets reflected with almost no loss of energy. Hence, soliton's scattering on a potential barrier is very elastic and thus the soliton behaves like a classical point particle. However, a soliton displays more interesting behaviour when it encounters a potential hole. Consider a classical point particle encountering a potential hole. Then, when the particle enters the hole, the hole speeds it up, no energy is lost and the point particle always gets transmitted. However, at low velocities, below a critical value, the scattering of solitons on a potential hole exhibits some aspects of a quantum-like behaviour in the sense that, sometimes, the solitons get reflected by the hole although most of the time they get trapped in the hole. Of course, such reflections are not possible for a classical point particle. A soliton with enough energy, i.e. with velocity above a critical value, can get out of the hole but it comes out with much reduced velocity as during the whole process it radiates some of its energy [1, 2].

  

In the present study, we look at various scattering properties of a topological soliton on an obstruction in two Lagrangian models. The Lagrangians are so constructed that, far away from the obstruction, the soliton in the two models looks exactly the same.

In the numerical part of this work we used square well potential barriers and holes of width 10. The simulations were performed using the fourth-order Runge–Kutta method of simulating the time evolution. We used 1201 points with a lattice spacing of $\mathrm{d}x = 0.01$. Hence, the lattice extended from $-60$ to 60 in the $x$-direction. The time step was chosen to be $\mathrm{d}t = 0.0025$. We used the absorbing boundary conditions.

### *1.1. Model 1: $\tilde{\lambda}(x)\varphi^4$ potential*

First we consider the model, in (1+1) dimensions $\mu = 0, 1$, defined by

$$\ell = \tfrac{1}{2}\partial_\mu\varphi\partial^\mu\varphi - U(\varphi) \tag{1}$$

with the potential

$$U(\varphi) = \tilde{\lambda}(x)(\varphi^2 - 1)^2,$$

where $\tilde{\lambda} = \lambda_0 + \lambda(x)$ and $\lambda(x)$ is a potential parameter which has been inserted into the Lagrangian to take into account the effects of obstructions, holes and barriers, and so is nonzero only in a certain region of space.

After varying the action, the equation of motion is

$$\partial_\mu\partial^\mu\varphi + 4\tilde{\lambda}(x)\varphi(\varphi^2 - 1) = 0. \tag{2}$$

This equation cannot be solved analytically because the potential has a spatial dependence. However, this equation can be solved numerically by placing the soliton in the region where $\lambda = 0$ and then evolving it from there.

Thus, the potential parameter $\tilde{\lambda}(x)$ has a constant value, $\lambda_0$, in the region where the soliton is located and far away from the position of the soliton $\tilde{\lambda}(x)\varphi(\varphi^2 - 1)$ is nearly zero as $\varphi \sim 0$. Moreover, as the system is fully relativistic, we can get an approximate time-dependent solution by simply boosting the static one. This gives us a soliton moving with velocity $u$. Thus (assuming that $x_0$ is nonzero and $t$ is small) we can put

$$\varphi(x, t) = \pm\tanh(\gamma\sqrt{(1 + \lambda_0)}(x - x_0 - ut)), \tag{3}$$

where

$$\gamma = \frac{1}{\sqrt{1 - u^2}}. \tag{4}$$

Here the plus and minus signs represent the kink and anti-kink solutions, respectively. At $t = 0.0$ the soliton is far away from the barrier/hole and the field configuration (3) describes the soliton very well. In what follows, we put $\lambda_0 = 0.0$ and so our initial conditions for the field and its time derivative are given by

$$\varphi(x, 0) = \pm\tanh(\gamma\sqrt{2}(x - x_0)) \tag{5}$$

$$\partial_0\varphi(x, 0) = \mp u\gamma\sqrt{2}\,\mathrm{sech}^2(\gamma\sqrt{2}(x - x_0)). \tag{6}$$

The energy density of the field is given by

$$\epsilon = \tfrac{1}{2}(\partial_0\varphi)^2 + \tfrac{1}{2}(\partial_1\varphi)^2 + (\varphi^2 - 1)^2. \tag{7}$$

### *1.2. Model 2: a $\lambda\varphi^4$ model with a position-dependent metric*

In this paper, we also consider the behaviour of a soliton in (1+1) dimensions when the potential parameter ($\lambda(x)$) arises in the spacetime metric, i.e. the metric is given by

$$g^{\mu\nu} = \begin{pmatrix} 1+\lambda(x) & 0 \\ 0 & -1 \end{pmatrix}.$$

The introduction of the spacetime metric makes the model more of a cosmological nature and therefore suitable for some cosmological considerations. The metric is Minkowskian in some regions and is different in some others (due to, say, the influence of some gravitational bodies).

Thus, we are putting the obstruction into the model in the same way as was done in [3] in the sine-Gordon case.

The action is now given by

$$s = \int \ell(\varphi, \partial_\mu\varphi)\,\mathrm{d}x\,\mathrm{d}t, \tag{8}$$

where $\ell$ is the Lagrangian density and $g$ is the determinant of the metric, i.e. $g(x)^{\mu\nu}$,

$$\ell = \sqrt{-g}\left[\tfrac{1}{2}\partial_\mu\varphi\partial_\nu\varphi g^{\mu\nu} - U(\varphi)\right] \tag{9}$$

with the potential still being given by

$$U(\varphi) = (\varphi^2-1)^2.$$

Note that the coefficient of the potential in $U(\varphi)$ is chosen to be 1, i.e. it is the same as in model 1 away from the obstruction. The equation of motion is now

$$(1+\lambda(x))\partial_0^2\varphi - \partial_1^2\varphi - \frac{1}{2\mid 1+\lambda(x)\mid}\partial_1\lambda(x)\partial_1\varphi + 4\varphi(\varphi^2-1) = 0. \tag{10}$$

The topological charge is independent of the metric and does not depend on the potential. The equation of motion (10) cannot be solved analytically because of the spatial dependence of the potential parameter. But, like before, a solitonic solution can be found by making the potential parameter constant, $\lambda(x) = \lambda_0$, and then use that solution as an initial condition to solve equation (10) numerically. Note that when $\lambda_0$ is constant equation (10) becomes

$$(1+\lambda_0)\partial_0^2\varphi - \partial_1^2\varphi + 4\varphi(\varphi^2-1) = 0. \tag{11}$$

The approximate time-dependent solution for the field is given by

$$\varphi(x,t) = \pm\tanh\left(\sqrt{\frac{2}{1-u^2(1+\lambda_0)}}(x-x_0-ut)\right). \tag{12}$$

Next we choose $\lambda_0 = 0.0$ and so the initial conditions are

$$\varphi(x,0) = \pm\tanh\left(\sqrt{\frac{2}{1-u^2}}(x-x_0)\right), \tag{13}$$

$$\partial_0\varphi(x,0) = \mp u\sqrt{\frac{2}{1-u^2}}\,\mathrm{sech}^2\left(\sqrt{\frac{2}{1-u^2}}(x-x_0)\right), \tag{14}$$

which are, in fact, the same as the initial conditions of model 1.

The energy density is then given by

$$\epsilon = \sqrt{g^{00}}\left[\frac{g^{00}}{2}(\partial_0\varphi)^2 + \frac{1}{2}(\partial_1\varphi)^2 + (\varphi^2-1)^2\right]. \tag{15}$$

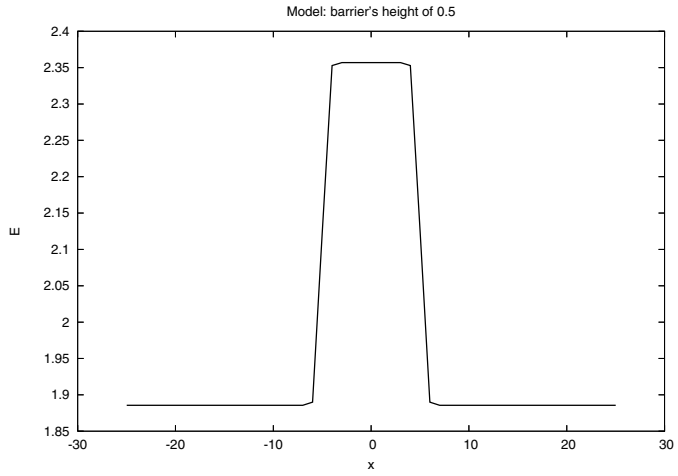


**Figure 1.** The potential barrier as seen by the soliton in the two models.

## 2. Barrier scatterings in both models

The scattering of a topological soliton on a potential barrier, in model 1, was found to be nearly elastic. However, in model 2, the scattering was found to be less elastic as, in this case, the soliton radiated away a small amount of its energy, although this radiated energy was very small (almost negligible) when the velocity of the soliton was far below its critical value. However, it increased as we sent solitons with higher velocities.

The shape of the potential barrier, as seen by the soliton, can be found by placing the soliton with a zero velocity at different positions and calculating its total energy. This has provided figure 1 which shows how a soliton would see a potential barrier of height 0.5 in both models.

However, performing numerical simulations we have found a difference between the two models. In model 1, the behaviour of a topological soliton resembles a classical point particle as only a very small amount of energy is being radiated out during the scattering process. However, in model 2, this amount of radiation is much larger and it increases as we increase the height of the barrier. Figures 2(*a*) and (*b*) show the time evolution of the position of the soliton (moving with velocity 0.8) for different barrier's heights in models 1 and 2, respectively. We see very clearly that in model 2 the soliton loses more energy (through radiation) and consequently leaves the scattering region with lower velocity. Not surprisingly, this effect grows with the increase in barrier's height in both models but is much more pronounced in model 2.

We have also found a small variation of outgoing velocity of the soliton as a function of its incoming velocity; again this effect is more pronounced in model 2. Figure 3 shows our results for a potential barrier of height $= 0.5$. Figure 4 indicates how in model 2 this variation (oscillation) gets more pronounced with the increase in the height of the barrier. Figures 3 and 4 exhibit the dependence of the outgoing velocity on the initial velocity for various values of the barrier heights ($\lambda_0$) in models 1 and 2. As we see from figure 3 (height $\lambda_0 = 0.5$) the soliton in model 2 loses more energy (i.e. the barrier distorts its shape more—leading to a greater loss of energy). We note the interesting oscillatory pattern of the curve corresponding to model 2 (in fact the curve for model 2 has also some oscillations, but their amplitude is so

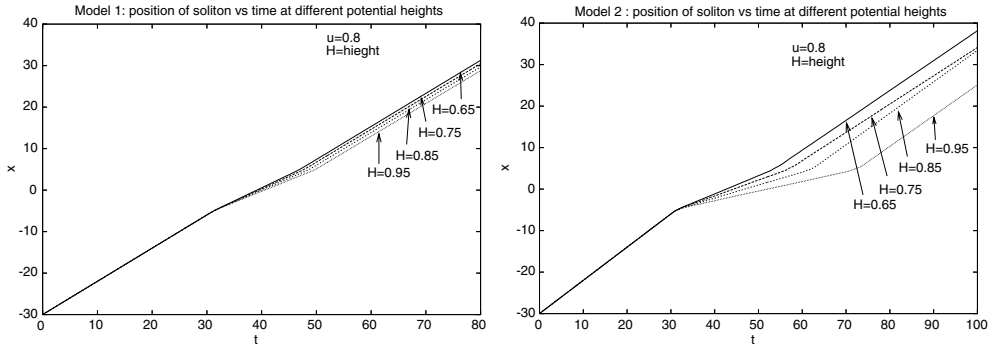


**Figure 2.** The position of the soliton versus time for various barrier's heights.

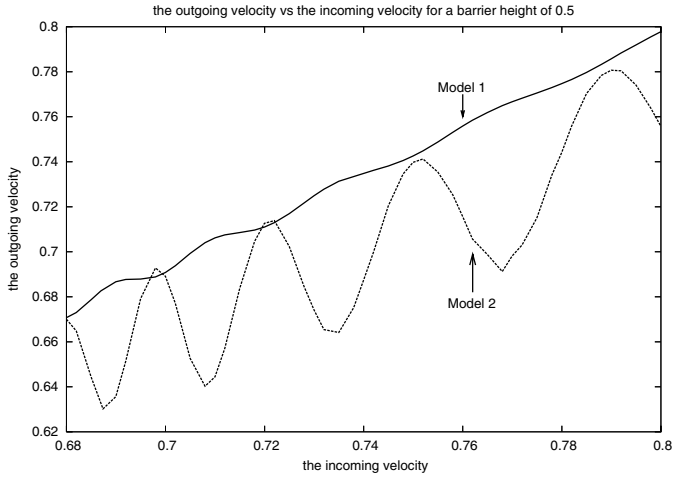


**Figure 3.** $v_{\text{out}}$ versus $v_{\text{in}}$ for a barrier of height 0.5 in the two models.

small that they are almost invisible). Hence, we have also looked at other values of $\lambda_0$ in model 2—the corresponding curves are shown in figure 4. The curves there clearly demonstrate that as the barrier height increases the amplitude of the oscillation increases and so does their frequency. We have no explanation of these oscillations at this stage and so, right now, we can only speculate as to their origin. However, it is clear that their origin probably resides in the interaction of the soliton with the radiation that was generated as the soliton entered the barrier; similar behaviour was observed in the sine-Gordon model for the soliton in the hole [2]; there the explanation involved such an interaction. At the same time, as shown in [1], similar oscillations in some relativistic models can be generated by taking initial solitons with slightly incorrect profiles (e.g. by forgetting to include the correct relativistic profile factors). Model 2 involves the variation of the metric and so is more sensitive to the variation of the soliton profile as it transverses the barrier. So, from this point of the view this variation is not so surprising. It is clear, moreover, that once the soliton is in the barrier region its velocity is modified by the barrier factor $\frac{1}{\sqrt{1+\lambda_0}}$. However, this fact, by itself, does not explain the oscillations which are probably generated as the soliton enters and leaves the barrier region.

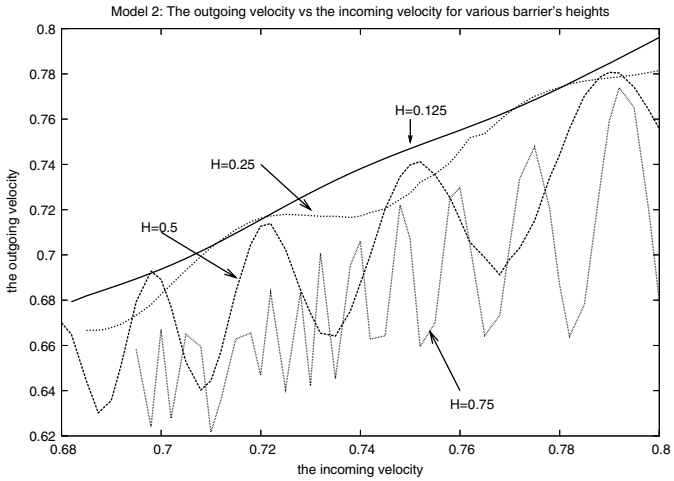


**Figure 4.** Model 2: $v_{\rm out}$ versus $v_{\rm in}$ for various barrier's heights.

The problem of the origin of the oscillation is still being studied by us and hope to be able to report on this in not too distant future.

### *2.1. Some analysis of our results*

We have found that the solitons behave in a similar way in the two models but that the differences from the behaviour of a point particle are more pronounced in model 2. This difference was found to be related to the oscillations of the kink corresponding to the change of its slope (i.e. the coefficient of $x$ in (3) and (12)). These oscillations are generated because the slope of the soliton changes as the soliton moves up the barrier. This encounter is somewhat sudden, the slope changes too much and so it starts oscillating. The soliton thus tries to readjust itself to the new value of the slope (corresponding to the new value of $\tilde{\lambda}$) and during this readjustment some of its kinetic energy is converted into oscillating energy. To test such an interpretation we divided the slope of the soliton before the interaction with the barrier over the slope of the soliton when it is at the barrier and then have plotted this ratio as a function of the incoming velocity. Figure 5 shows the plot of the ratio for a barrier of height 0.5 in the two models. From the figure one can see that below the critical value, i.e. when the soliton gets reflected, the ratio of the two slopes is small and increases steadily as the soliton velocity increases. However, above the critical value, i.e. when the soliton gets transmitted, the ratio in model 2 increases steadily, but only slightly this time, while in model 1 it is almost constant.

Furthermore, we have also studied the range of the oscillations and the average square of their frequency. We have found that above the critical value the average square of the frequency is directly proportional to the incoming velocity. This demonstrates that the energy radiated, which is proportional to the square of the frequency, increases as we increase the incoming velocity. This supports our argument that the soliton oscillates and that a fraction of its energy is converted into vibrating energy.

The range of the oscillation (see the appendix for the derivation) is given by

$$\delta \sim \frac{S_1 - S_2}{S_2\sqrt{S_1^2 - 1}}, \tag{16}$$

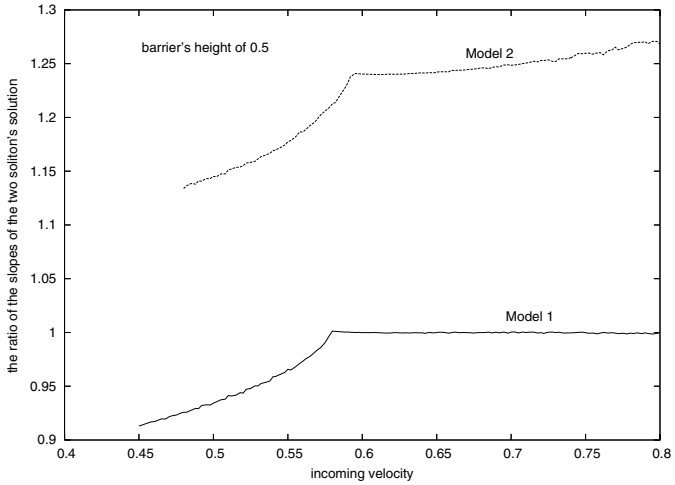


**Figure 5.** The ratio of the slopes of soliton's solutions versus incoming velocity in the two models.

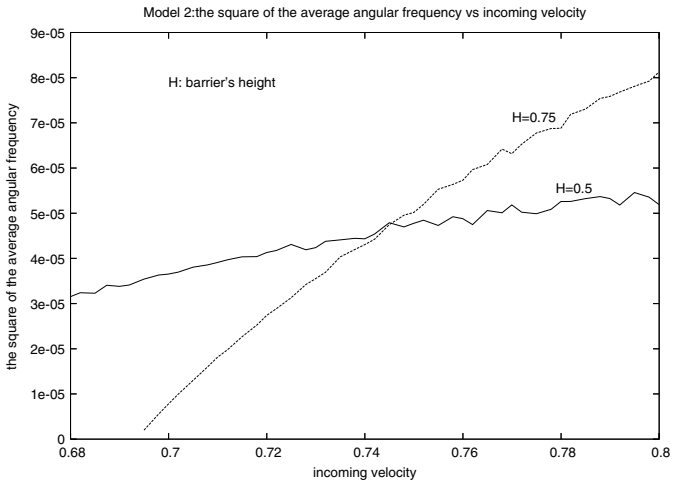


**Figure 6.** $\omega^2$ as a function of $v_{\text{in}}$ in model 2.

where $S_1$ is the slope of the soliton before and after the barrier. $S_2$ is the slope at the barrier. This result holds in the limit when the difference between the slopes is very small (so that we can make the approximation that $\sin(\delta) \sim \delta$). The average of the frequency, $\omega$, is given by

$$\omega = \frac{\delta}{\Delta t}, \tag{17}$$

where $\Delta t$ is the time spent by the soliton at the barrier. Figure 6 illustrates the relation between the average square of the frequency and the incoming velocity, at heights 0.5 and 0.75. The figure shows that, as the incoming velocity increases, the oscillations increase and so does the radiated energy.

We have found that the difference in oscillations and obviously in the behaviour of solitons in the two models is due to the different energy, i.e. mass, they have at the barrier. The more

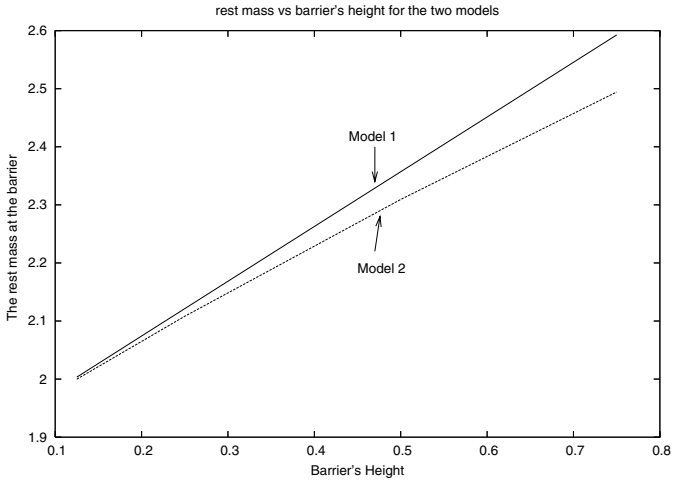


**Figure 7.** Rest mass versus barrier's height in the two models.

**Table 1.** Soliton's critical velocities for potentials of various heights.

| Model number | $\lambda_0 = 0.125$ | $\lambda_0 = 0.25$ | $\lambda_0 = 0.5$ | $\lambda_0 = 0.75$ |
|---|---|---|---|---|
| Critical velocities | | | | |
| Model 1 | ∼0.34 | ∼0.45 | ∼0.58 | ∼0.66 |
| Model 2 | ∼0.358 | ∼0.463 | ∼0.596 | ∼0.695 |

massive the soliton is the fewer oscillations it makes during the interaction. There is a greater sensitivity of the potential for less massive solitons than for the heavy ones. The mass of a static soliton, $M_{\rm rest}$, is given by the integral over the energy density:

$$M_{\rm rest} = \int_{-\infty}^{\infty} \left[ \frac{1}{2}\varphi_x^2 + U(\varphi) \right] {\rm d}x = \frac{8\sqrt{1+\lambda_0}}{3\sqrt{2}}. \tag{18}$$

When the soliton is far from the obstruction $\lambda_0 = 0.0$ and so its energy, i.e., mass $M = 1.88557$ in both models and this is exactly what was found numerically. For a moving soliton it is given by

$$E = \int_{-\infty}^{\infty} \left[ \frac{1}{2}\varphi_t^2 + \frac{1}{2}\varphi_x^2 + U(\varphi) \right] {\rm d}x = \frac{M}{\sqrt{1-u^2}}, \tag{19}$$

where $u$ is the speed of the soliton.

Figure 7 shows a plot of the soliton rest mass as a function of the height of the barrier in the two models.

We have also looked at the values of critical velocities in both models. In table 1, we give these values for various heights of the potential in both models. It is clear that the critical velocities in model 2 are greater than those of model 1. That is very understandable since to reach the values of the rest masses in model 1, one needs a larger value of the gamma factor which thus leads to smaller critical velocities.

Figure 8 shows a plot of the critical velocity as a function of the height of the barrier in the two models.

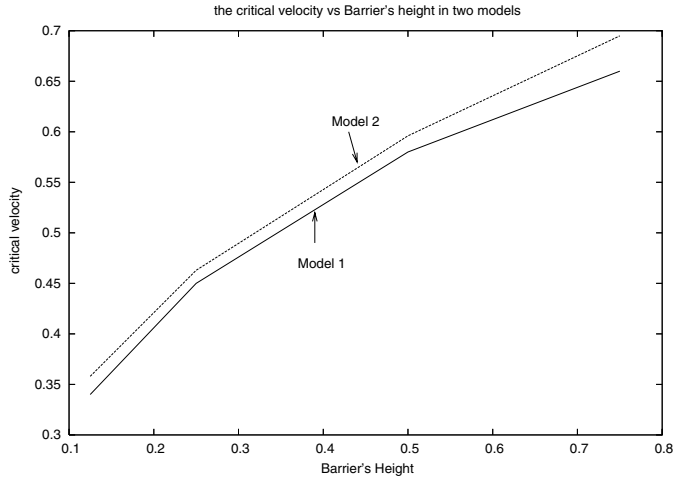


**Figure 8.** Critical velocity as a function of barrier's height in the two models.

A soliton is an extended object. However, in a particle picture, the soliton rest mass energy is

$$E = Mc^2, \qquad \text{with} \qquad c = 1 \tag{20}$$

where $M$ is the mass of the soliton. Thus, in the particle picture, if a soliton is sent towards a potential barrier with a critical velocity, $u_{\rm cr}$, then it would almost have enough energy to climb up the potential barrier. In this situation the soliton critical energy, $E_{\rm cr}$, has to be very close to the soliton rest mass. In a classical particle picture if the kinetic energy of the soliton is completely converted into the potential energy, the soliton will forever stay at the top of the barrier because the difference between the critical energy and the rest mass energy is zero. However, practically, the difference is very small and if we let the difference to be around $\sim x$, where $x$ is a very small number, then

$$E_{\rm cr} - M_{\rm rest} \sim x,$$

where $M_{\rm rest}$ is the rest mass of the soliton at the top of the barrier and we expect $x$ to be very small:

$$E_{\rm cr} = \frac{M}{\sqrt{1 - u_{\rm cr}^2}}, \tag{21}$$

where $M$ is the rest mass of the soliton when it is far away from the potential which was found to be 1.88557. Thus, the critical velocity is given by

$$u_{\rm cr} = \sqrt{1 - \left(\frac{M}{M_{\rm rest} + x}\right)^2}. \tag{22}$$

In model 2, the rest mass of the soliton at a barrier of height 0.5 was found to be 2.3093, see figure 7. Putting $x = 0.02$ we estimate the critical velocity as

$$u_{\rm cr} = \sqrt{1 - \left(\frac{1.88557}{0.02 + 2.309}\right)^2} \sim 0.592,$$

which is in excellent agreement with what was found numerically (see figure 8 where it is given by 0.596).

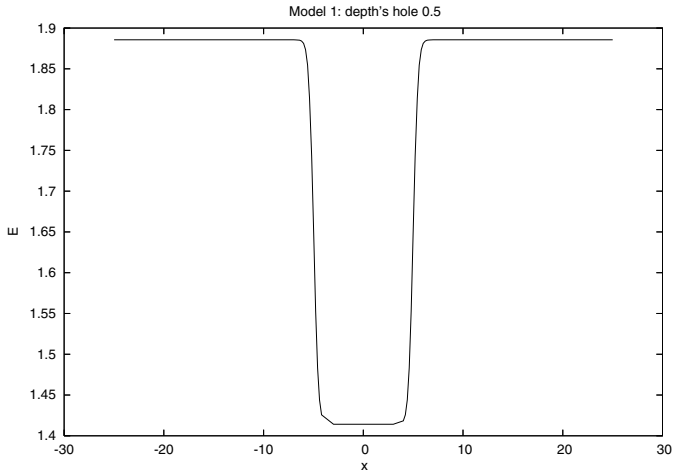


**Figure 9.** The potential hole as seen by the soliton.

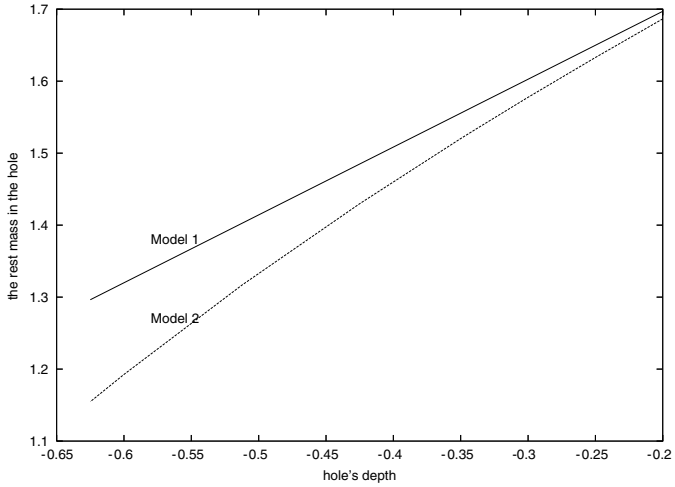


**Figure 10.** Soliton rest mass versus hole's depth in the two models.

## 3. Hole scattering

A classical particle is always transmitted through a potential hole. However, numerical simulations of the scattering of topological solitons [1, 2] have shown that, when the potential hole is deep enough, there is a critical velocity below which the soliton gets trapped in the hole. Moreover, just below this critical velocity the soliton can get reflected by the hole, thus showing behaviour which is more like of a quantum object. Of course, there is nothing 'quantum' about it—the soliton gets trapped in the hole and interacts with the radiation waves that it has sent out and . . . , occasionally, for very specific values of its velocity this interaction leads to the back escape of the soliton which looks like its reflection by the hole.

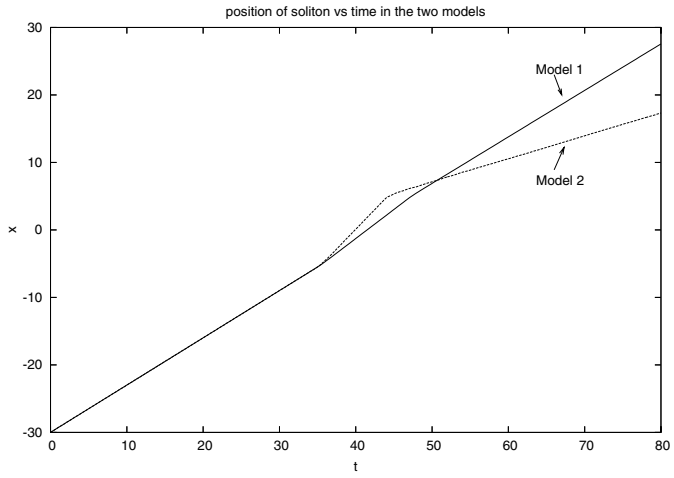


**Figure 11.** The position of the soliton versus time in the two models.

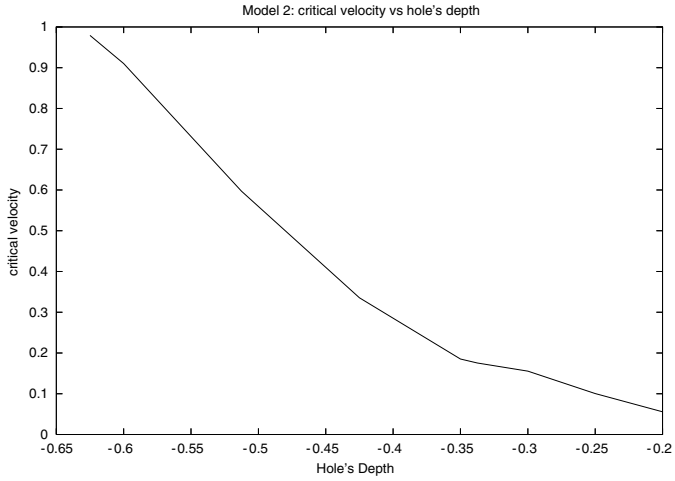


**Figure 12.** Critical velocity versus hole's depth.

In the present work, we have also performed many simulations of the scattering of solitons on the holes for the two models and have seen the same behaviour. Like in [1] we have found that the soliton gets trapped in the hole and that it can get reflected. In all cases it radiates some energy, hence if it comes out of the hole its velocity is lower than at its entry.

In our work, we placed a square hole of width 10 at the same position as the barrier in the previous simulations. Again, when the soliton is far away from the hole its rest mass $M = 1.88557$. When the soliton approaches the hole of $-0.50$ depth, the hole appears as in figure 9 with no difference between the two models. In figure 10, we present a plot of the soliton rest mass as a function of the hole depth.

As when the soliton is in the hole it has a lower rest mass in model 2 than in model 1, the soliton in model 2 has more 'spare' energy and so it radiates more energy. Figure 11 shows

how the position of a soliton moving with a velocity of 0.65 evolves in time in the two models. From the figure we can see that the loss of energy in model 2 is higher than in model 1.

Incidentally, model 2 has one more interesting scattering property. We have found that for a hole depth just below $-0.625$, the solitons are always trapped. Hence there is no critical velocity. For example at a hole depth of $-0.625$ the critical velocity is $\sim 0.97$. Figure 12 shows a plot of the critical velocity as a function of the depth of the hole for model 2.

## 4. Conclusion

We have constructed two models involving two different ways of introducing a localized obstruction in the $\lambda\varphi^4$ model and on the scattering properties of solitons on obstructions in such models. In the first model the coefficient $\lambda$ was made to be a function of the space variable $x$, in the second one the obstruction was introduced through the modification of the metric. The scattering properties of solitons in both models were very similar, and quite similar to what was seen in the sine-Gordon model; however, when we looked at the details of the scattering we did spot some differences. The scattering in the first model was more elastic; in each case we related this to the fact that the solitons had different rest mass energies at the obstruction. The origin of such a mass difference in the two models is due to the change of the soliton slope as the soliton climbs the obstruction. Due to this difference the scattering of the soliton on the obstruction was more elastic in model 1 than in model 2

When we looked at the scattering by the hole we found that, like in the sine-Gordon case, the scattering was much more inelastic in both models with model 2 generating much more radiation. In fact, in model 2, for the holes sufficiently deep the soliton was completely trapped in them, i.e. we could not find any velocity above which the soliton could escape from the hole.

The sine-Gordon model is integrable and the $\lambda\varphi^4$ one is not. So, naively, we could expect more differences in the scattering of their solitons. However, this is not borne out by our numerical results which suggest that the phenomena observed by us are not really related to the integrability (or not) of the models. The only significant difference seen by us is the amount of the emitted radiation which, as expected, is larger in the $\lambda\varphi^4$ model.

The question then arises whether all these results are very generic, i.e., hold in most (1+1)-dimensional solitonic models or are just the property of the $\lambda\varphi^4$ model. This problem is currently under investigation. Moreover, we also need to obtain some analytical understanding of the observed results. In the sine-Gordon model this was achieved [2] by the introduction of effective variables describing the oscillation of the vacuum in the hole—very much in the same way Goodman *et al* [5] explained the results of Fei *et al* [4]. We plan to look for a similar explanation in this case too.

## Appendix

Consider two kink states having different inclination angles as shown in figure A1 and let $S_1$ be the slope of the kink when the soliton is not interacting with the barrier and $S_2$ is the slope of the kink when it is at the barrier. When the soliton hits the barrier and gets transmitted its slope is greater than its initial value, i.e., when it is away from the barrier. This is shown in figure 5.

Let $\delta$ be the angle between the two kinks and $\theta$ be the angle between the vertical line and the kink of slope $S_1$. Then from the above figure one can, approximately, deduce the following

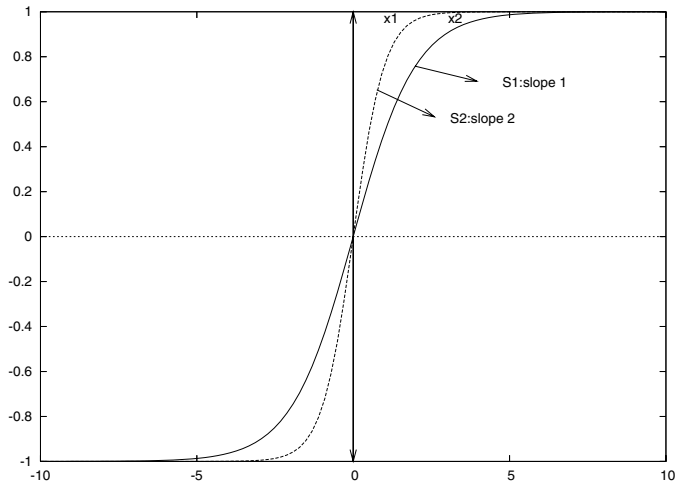


**Figure A1.** Two kink states at different inclination angles.

algebraic relations:

$$\cos\theta = \frac{1}{S_1}, \qquad \cos(\theta - \delta) = \frac{1}{S_2}, \qquad x = x_1 + x_2,$$
$$x^2 = S_1^2 - 1, \qquad \sin\theta = \frac{x}{S_1}.$$

Using $\cos(\theta - \delta) = \cos\theta\cos\delta + \sin\theta\sin\delta$, and substituting the above algebraic relations into this identity, one gets

$$\frac{1}{S_2} = \frac{1}{S_1}\cos\delta + \frac{x}{S_1}\sin\delta. \tag{A.1}$$

Because the angle $\delta$ is small, one can make the approximations, i.e., $\cos\delta \sim 1$ and $\sin\delta \sim \delta$.

After some simple algebra one obtains equation (16), i.e.,

$$\delta \sim \frac{S_1 - S_2}{S_2\sqrt{S_1^2 - 1}}. \tag{A.2}$$

## References

[1] Piette B M A G, Zakrzewski W J and Brand J 2005 *J. Phys. A: Math. Gen.* **38** 10403–12
[2] Piette B M A G and Zakrzewski W J 2007 *J. Phys. A: Math. Gen.* **40** 329–46
[3] Javidan K. 2006 *J. Phys. A: Math. Gen.* **39** 10565–74
[4] Fei Z, Kivshar Yu S and Vazquez L 1992 *Phys. Rev.* A **45** 6019–30
[5] Goodman R H and Haberman R 2004 *Physica* D **195** 303–23